

Potential Flows in a T-Junction

Aisling Heanue, James Herterich

June 2021

1 Abstract

We use the Lightning Laplace Solver, a new solver for Laplace's equation, to obtain a model for fluid flow in a T-junction, where fluid enters from the top and splits into two directions. We compare this model with the stagnation point flow to investigate how well it approximates this flow. We find these models agree more for T-junctions with rounded corners than for those with sharp corners, where there is a greater difference between their results.

We calculate small particle paths in the T-junction and find that particles starting closer to the edge of the junction exit at a higher point and spend less time in the pipe. We find that particles with lower Stokes numbers follow the fluid flow better and exit at a higher point, and all particles with a Stokes number greater than 0.1 will collide with the bottom wall before exiting.

We vary the radius of the corners to see how it affects the particle paths and find it has a weak effect on the final positions and travel times of particles in this flow.

2 Introduction

2.1 Stagnation point flows

We describe a stagnation point flow as a 2-dimensional incompressible and irrotational fluid flow bounded by solid walls in a T-junction geometry, like in Figure 1. We model potential flow. The position of the stagnation point depends on the flow entry and exit points. In Figure 2 this is at the point $(0,0)$. The classical representation of stagnation point flow [4] has the complex potential

$$w = kz^2 = kx^2 - ky^2 + 2ikxy, \quad y > 0 \quad (1)$$

and has a stagnation point where no fluid flow takes place at $(x, y) = (0, 0)$. This representation is limited in that it imposes only one of the solid wall boundaries (at $y = 0$), and does not represent other boundary conditions. Since this flow is irrotational and incompressible, its potential function satisfies Laplace's equation,

$$\nabla^2 w = \frac{\partial^2 w}{\partial x^2} + \frac{\partial^2 w}{\partial y^2} = 2k - 2k = 0 \quad (2)$$

We derive the fluid velocity of the stagnation point flow by differentiating w with respect to x and y and taking the real part to get the velocities in the x - and y -directions respectively.

$$(u, v) = \text{Real}\left(\frac{\partial w}{\partial x}, \frac{\partial w}{\partial y}\right) = \text{Real}(2kx + 2iky, -2ky + 2ikx) = (2kx, -2ky) \quad (3)$$

In this investigation, we analyse the claim that this flow is similar to flow entering a pipe and reaching a T-junction[3]. We assume the flow in the T-junction will be incompressible and irrotational, so it will be a potential flow that satisfies Laplace's equation. This allows us to use a solver for Laplace's equation to obtain its potential function for the boundary conditions of a T-junction. We

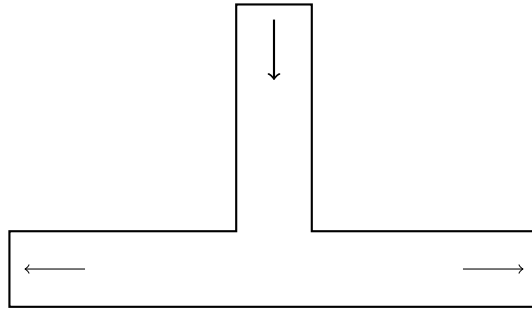


Figure 1: The T Junction

use a new solver for Laplace's equation that allows us to obtain the complex potential function for potential fluid flows. We compare this function with Equation 1 and determine the suitability of w as an approximation of potential flow in a T-junction.

We introduce small particles travelling through the pipe and investigate what effect the drag force of the fluid on them has on their trajectories. We vary the Stokes number of this particle to show the effect this has on where it exits the pipe and how long it spends travelling through it. We determine whether a particle collides with a wall or exits in the main fluid body and the residence time of the particle in the system. We compare the paths of these particles with the streamlines to see how well the particles follow these lines. We consider Stokes numbers between 0.001 and 0.1 for this.

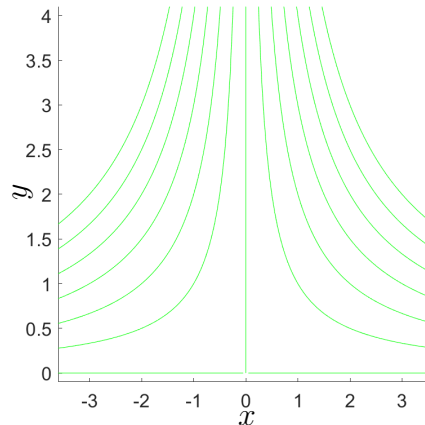


Figure 2: Streamlines of a stagnation point flow

2.2 The Lightning Laplace Solver

To calculate the complex potential of different flows, we use the Lightning Laplace Solver[1]. This solves Laplace's equation in polygonal or circular boundaries subject to Dirichlet or homogeneous Neumann boundary conditions. As potential flow may be described as such, the solver is suitable for our application. The real part of the solution represents the equipotential function and the imaginary part the streamlines.

The inputs accepted by the solver are P and g , where P is an ordered list of points used to define line segments and circular arcs that make up the boundary, and g is the Dirichlet boundary condition for each side of the boundary. If the value given for this condition is not numeric (or entered as 'NaN'), the solver imposes the homogeneous Neumann boundary condition there instead, so the boundary is treated as a solid barrier.

The solver calculates a solution to Laplace’s equation by finding sets of complex coefficients $\{a_j\}$ and $\{b_j\}$ such that the equation

$$r(z) = \sum_{j=1}^{N_1} \frac{a_j}{z - z_j} + \sum_{j=0}^{N_2} b_j (z - z_*)^j \quad (4)$$

satisfies the given boundary conditions. Here, z is the complex coordinate $x + iy$, and $\{z_j\}$ and z_* fixed points inside and outside the boundary, respectively. $\{z_j\}$ are taken to be singularities of the equation which are clustered exponentially near each vertex of the boundary. These are the red points in Figures 3 and 4. The first series allows $r(z)$ to be approximated accurately near the corner vertices with convergence $\|f - r_n\| = O(\exp(-C\sqrt{n}))$ because of how $\{z_j\}$ are chosen by the solver.[2]. The second sum uses the fact that polynomials can be used to approximate smooth functions in the plane.

We modify the solver to allow it to display streamlines instead of equipotential lines. Sample outputs of both functions of the Laplace Solver are shown below. Due to limitations with how contour maps are calculated in MATLAB, the streamlines are only displayed on one side of the junction in Figure 4.

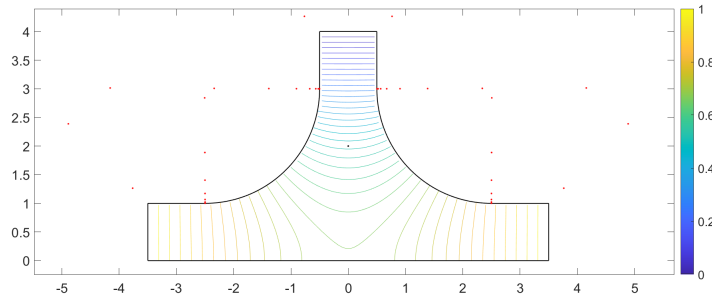


Figure 3: Equipotential lines output of Laplace Solver

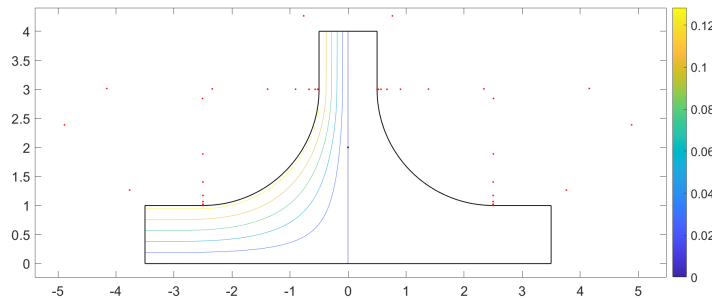


Figure 4: Streamlines output of Laplace Solver

2.3 The T-Junction

The classical T-junction is a pipe with one inlet and two outlets in opposite direction. These meet in a junction with a T shape, as depicted in Figure 1. Each wall of this pipe is treated as a solid boundary, and the outlets are given a positive Dirichlet boundary condition or potential difference pd . The inlet is given a boundary condition of zero. These are real numbers to indicate a potential difference across which fluid flows.

We also consider a T-junction with rounded corners at the turn with arc radius r to investigate whether altering the radius of these corners affects the potential function from the Laplace Solver.

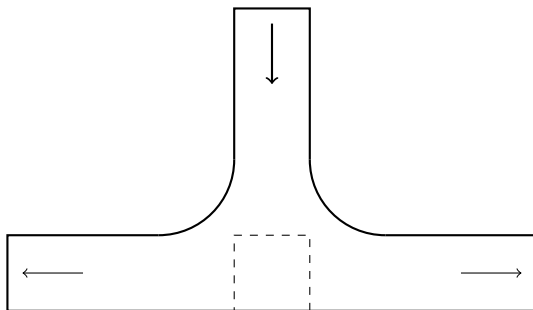


Figure 5: T-Junction with corner radius 1 unit, with comparison region highlighted

The pipes are each 3 units long, and we vary r between 0 and 2 units, where a radius of zero means there are sharp corners.

3 Methods

3.1 Comparing the T-Junction to the Stagnation Point Flow

We use the Lightning Laplace Solver to solve the fluid problem given by [state the problem: geometric boundary and potential difference]. We show the equipotential lines and streamlines in Figures 3 and 4 respectively. We obtain the complex potential functions for these flows, given by $f(x, y)$. In order to compare the stagnation point flow potential, w , with the computed f of the Laplace solver, we consider the square region at the intersection of the junction with side length 1 unit (Figure 5).

We know that $w(0, 0) = 0$ but the potential flow given by f is unique up to an additive constant. To minimise the error, f is adjusted such that $f(0, 0) = 0$ by subtracting $f(0, 0)$ from f . The value of k is chosen to minimise the difference between f and w at some point \mathbf{x}_0 in this region. Different values for \mathbf{x}_0 are considered to minimise the overall error.

We measure $|f(x, y) - w(x, y)|$ at 5000 evenly distributed points in the region and divide the sum by the total number of points to obtain the average error. We repeat this for different values of r and pd to investigate their effect on the error. We find that values of \mathbf{x}_0 closer to the bottom boundary produce less consistent results for the error as shown in the comparison in Figure 6. Note that \mathbf{x}_0 is expressed as the complex value $x + iy$ in these figures.

We find that the error scales linearly with pd , which is shown in Figure 7. As r is decreased, the error goes up and the stagnation point flow becomes a less accurate approximation for the potential function.

3.2 Calculating Particle Paths in a T-Junction

In the previous section we observed the differences in stagnation point flow by appropriately treating all boundary conditions. This affects systems that depend on that flow, such as transport of colloidal particles.

Particles in a steady flow at the position $\mathbf{x}_p = (x_p, y_p)$ are transported by hydrodynamic forces such as drag due to the fluid viscosity[3], with motion governed by

$$St \ddot{\mathbf{x}}_p = \frac{C_D}{2} (\mathbf{u} - \dot{\mathbf{x}}_p) |\mathbf{u} - \dot{\mathbf{x}}_p| \quad (5)$$

where $\mathbf{u} = (u, v)$ is the flow velocity of the fluid. C_D is the drag coefficient between the fluid and the particle, and St is the Stokes number of the particle. The x - and y -components are given by 2nd

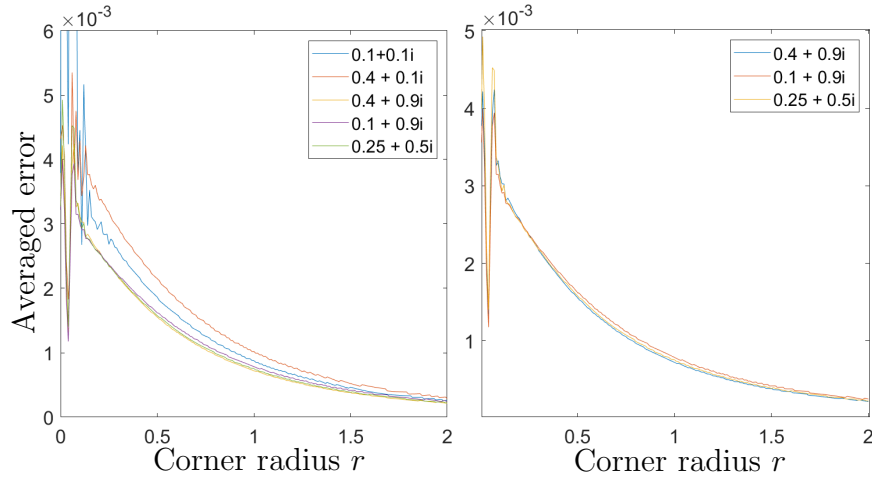


Figure 6: Error values agree better when some \mathbf{x}_0 are omitted

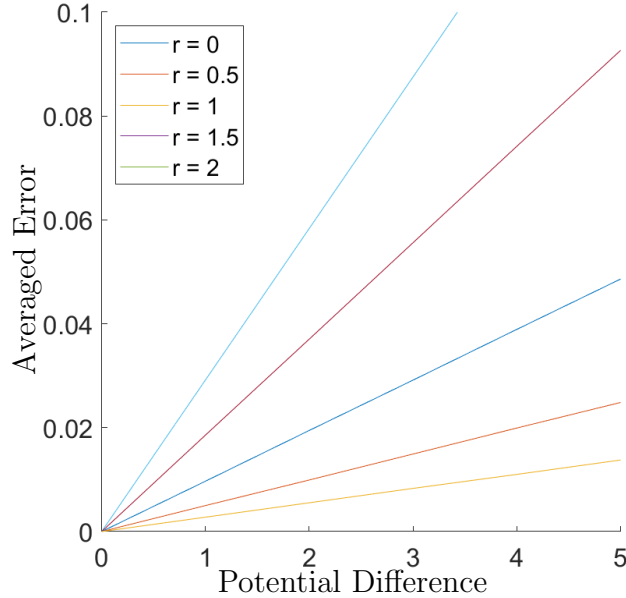


Figure 7: Averaged error scaling linearly with pd for several r

order coupled ordinary differential equations.

$$\begin{aligned}\ddot{x}_p &= \frac{C_D}{2St}(u - \dot{x}_p)|\mathbf{u} - \dot{\mathbf{x}}_p| \\ \ddot{y}_p &= \frac{C_D}{2St}(v - \dot{y}_p)|\mathbf{u} - \dot{\mathbf{x}}_p|\end{aligned}\tag{6}$$

Other forces on the particle may be important, including the drag due to a pressure gradient on the particle surface, mass force from acceleration of the fluid by the particle, lift caused by particle or fluid rotation, gravity, and lubrication forces as the particle approaches a wall[3]. We assume that the drag force is the dominant force for the purpose of this investigation.

We integrate these equations using MATLAB's ode45 function from a starting point at the entrance to the T-junction, tracking the particle paths as they were carried by the fluid flow. We use regular equispaced points along the inlet as starting points, and the initial velocities were assumed to be the

velocity of the fluid at that point.

We consider two different cases for the value of the function \mathbf{u} . The first is given by the stagnation flow, $(u, v) = (2kx, -2ky)$, where k is chosen to match a potential difference of 1 from inlet to outlet.

For the second case, we took a numerical finite difference approximation of the potential function $\varphi = \text{Re}(f)$, where f is given by the Lightning Laplace Solver, with respect to x and y to obtain u and v respectively.

We plot the particle paths alongside the streamlines, and compare it to the particle paths and streamlines given by the stagnation point flow. As discussed, the streamlines of the stagnation point flow do not take into account all walls of the T-junction. The results for some values of r and St are shown in Figure 8.

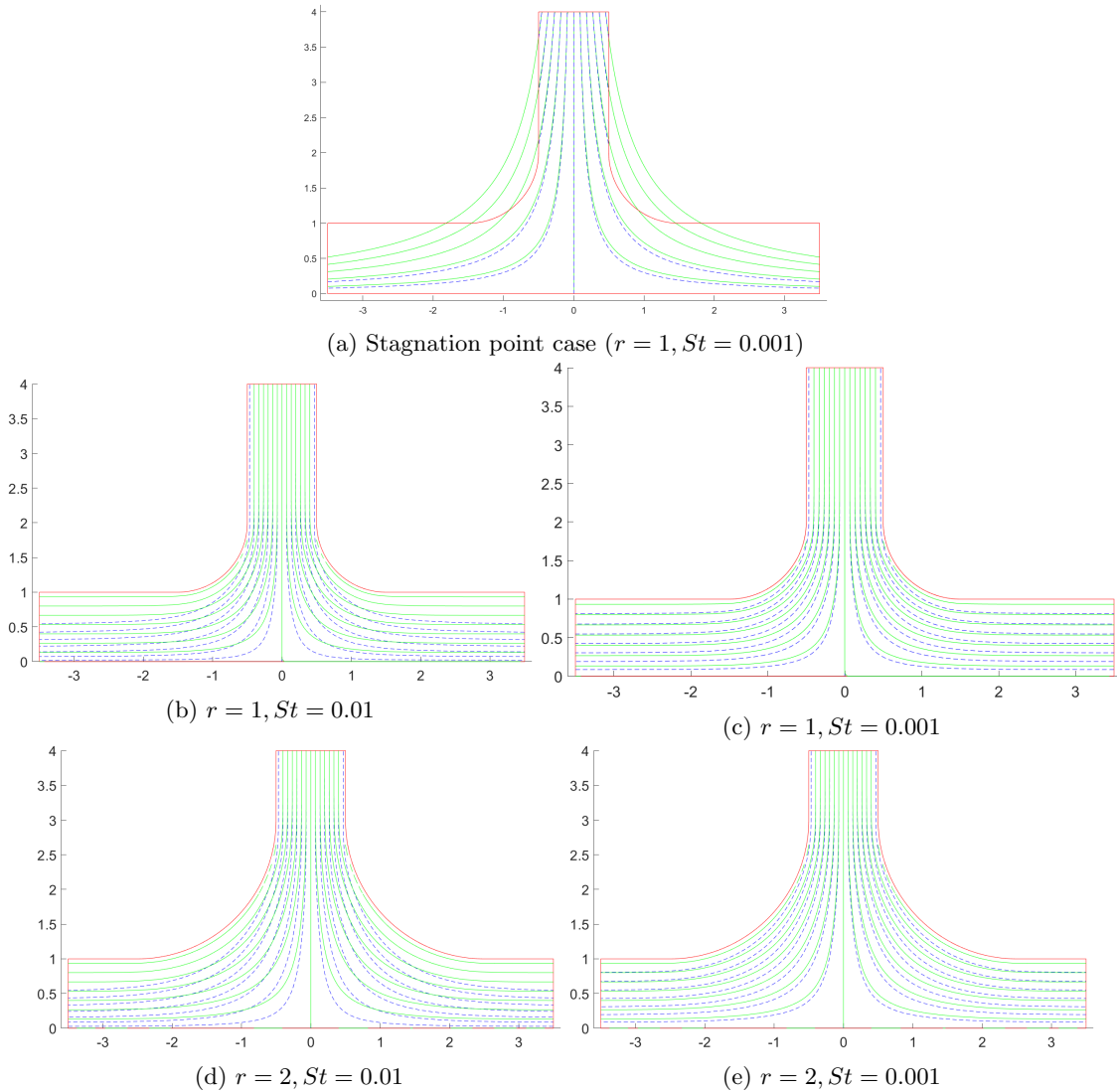


Figure 8: Streamlines (green) and Particle Paths (blue) for different r and St using the Lightning Laplace Solver

3.3 Investigating particle paths for different Stokes numbers and corner geometries

We look at the effect changing the geometry of the T-junction and the Stokes number has on the particle paths, and at what point they exit the pipe. We show the exit point y against the entry point x_0 for a given value of C_D , St and pd in Figure 9. We consider only x_0 values on the right hand side of the pipe since the flow is symmetric around the y -axis. This is repeated for different r values. We consider a range from 0 to 0.5 for x_0 . Figure 9 obtained using the values 1 for C_D , 0.007 for the Stokes number, and 1 for pd .

In Figure 9 we see a significant difference between the exit and entry points for stagnation point flow and potential flow via the Lightning Laplace Solver. Greater values in exit point y are obtained and for a larger range of entry points x_0 . However, only a weak dependence on r is evident.

We analyse the maximum point in the T-junction from which particles exit by considering particles starting close to one side of the inlet. We plot this position, y , against the Stokes number of the particle, St , for different r values with $pd = 1$ (Figure 10)

In Figure 10, the dependence on r is weak for small Stokes numbers, but as Stokes numbers increase a clear dependence emerges.

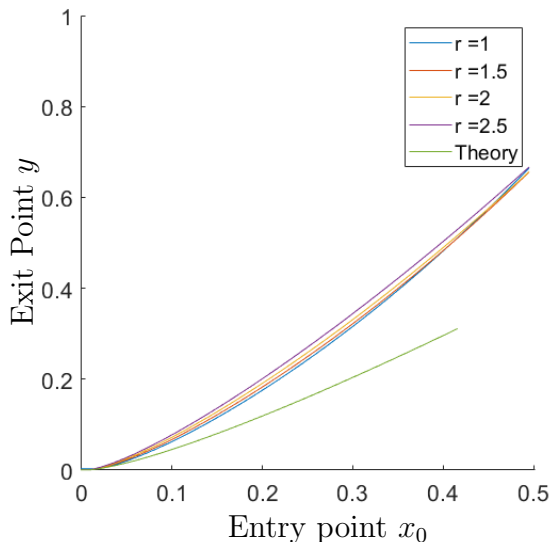


Figure 9: Ending position of particles vs entry points x_0 of the T-junction

3.4 Investigating travel times of particles

We find the travel times of the particles based on where they entered the pipe for various radii r . We show in Figure 11 the residence time for Stokes number 0.007 and potential difference 1. Particles closer to the side will exit the pipe sooner because they have a shorter distance to travel. Particles near the centre of the pipe will spend longer there as they have to travel a further distance and their paths will come close to the stagnation point, where the flow is the slowest. The value of r is seen to weakly affect the travel times here.

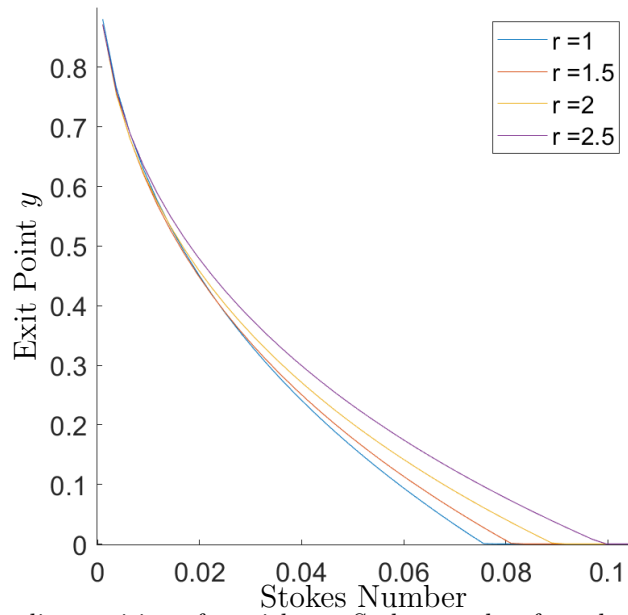


Figure 10: Highest ending position of particles vs Stokes number for values of r for the T-junction

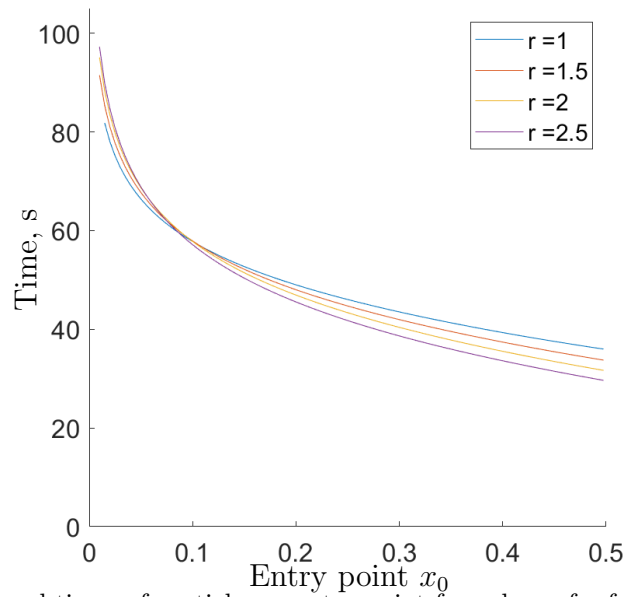


Figure 11: Travel times of particles vs entry point for values of r for the T-junction

3.5 Two entry flows

We alter the potential at the outlets to change the left outlet to an inlet, and to see how it would affect the particle paths near the junction. We set the boundary at the top and right to have Dirichlet boundary conditions of 0 and 5 respectively. The particle paths are plotted for several values of the boundary condition at the left inlet (Figure 12).

When the potential difference between the top and left is zero, the flow at both of these sides will have similar energies, and the flows will meet at the junction before exiting the pipe together. As the potential difference increase, the flow becomes less symmetric at the junction, and the particles entering from the left are pushed down to the bottom wall.

We look at what point in the outlet the two flows meet to determine how the potential difference between the outlets affects the amount the flow from the left is confined to the bottom by the top flow. For a pipe with corner radius 2 and top potential equal to zero, we vary the potential at the left between 0 and 2.5 for potentials at the right between 3 and 5, and plot the point where the flows meet in Figure 13. We find that a higher potential difference between the left and right exits leads to the flows meeting at a higher point at the exit, and a lower potential at the right exit point means there is a lower potential difference between the left and right so that top flow is able to dominate the flow and confine the flow from the left to the bottom wall more easily. All the particles from the left wall are confined to the bottom wall for a sufficiently high left potential, which can be seen in Figure 12c.

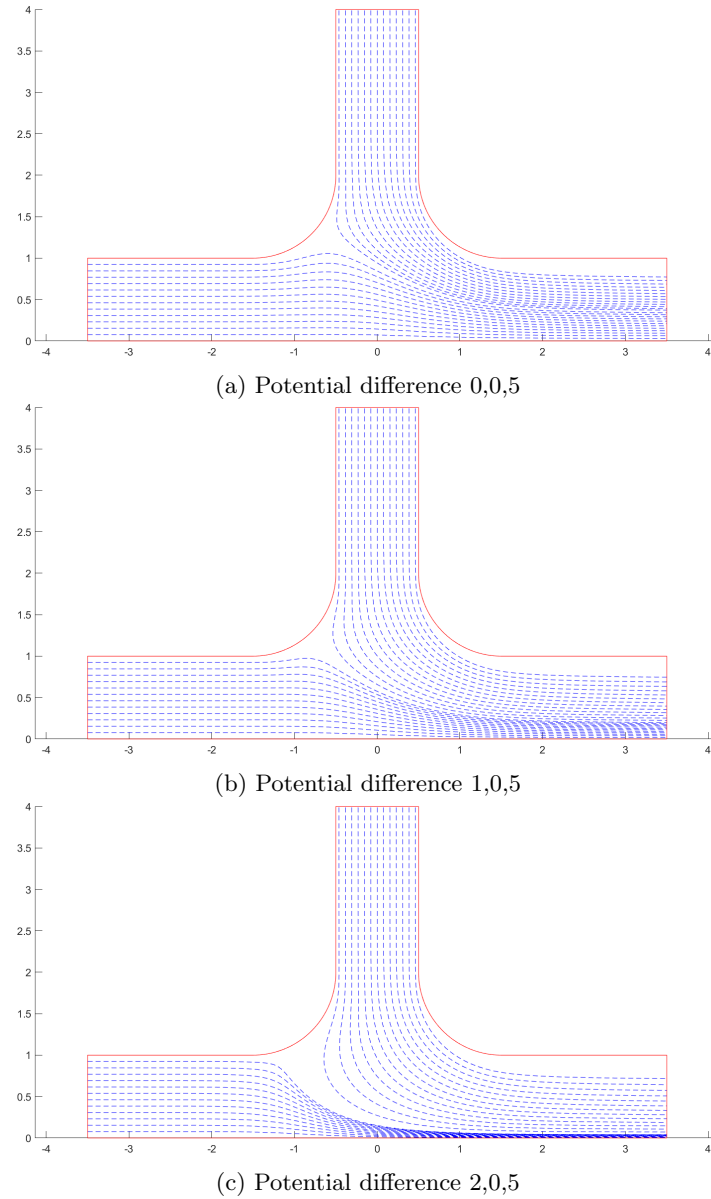


Figure 12: Particle paths for flows with given potentials at the left, top and right outlets

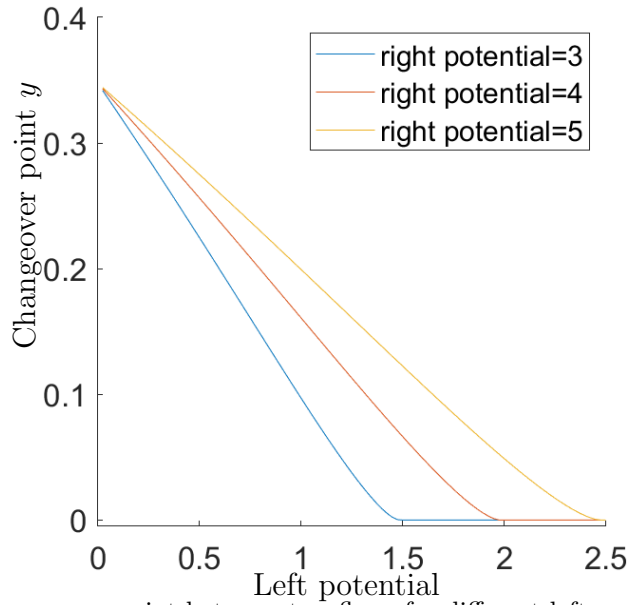


Figure 13: Changeover point between two flows for different left and right potentials

4 Conclusion

We used a new solver for Laplace’s equation, the Lightning Laplace Solver to compare the streamlines of a flow through a T-junction with those of the stagnation point flow, and found that this flow was not a good approximation of sharp corner junctions. We looked at the effect of the T-junction’s shape on the paths of small particles in this flow, and saw that their exit points were weakly affected by the arc radius of the corners. We found that the particles’ Stokes number had a larger impact on where they ended up after being carried by the flow. We saw that particles which started closer to one side of the inlet exited at a higher point and spent less time travelling through the junction. Finally, we altered the potential at one of the outlets to study the effect it had on particle paths near the junction, and demonstrated that when two flows merged at the junction, the inlet particles with a lower potential difference would be confined to a narrower section by the faster flow.

References

- [1] Abinand Gopal and Lloyd N. Trefethen, New Laplace and Helmholtz solvers, PNAS 116, no. 21 (2019) pp. 10223-10225
- [2] Schwab C., p- and hp-finite element methods. Theory and applications in solid and fluid mechanics. Oxford University Press (1998)
- [3] Vigolo, Daniele, et al. ”An experimental and theoretical investigation of particle-wall impacts in a T-junction.” Journal of fluid mechanics 727 (2013), pp. 236-255
- [4] Richard E. Meyer, Introduction to Mathematical Fluid Dynamics (2012) pp. 19-21